Orbital character variation of the Fermi surface and doping dependent changes of the dimensionality in $BaFe_{2-x}Co_xAs_2$ from angle-resolved photoemission spectroscopy

S. Thirupathaiah,[1] S. de Jong,[3] R. Ovsyannikov,[1] H.A. Dürr,[1] A. Varykhalov,[1] R. Follath,[1] Y. Huang,[3] R. Huisman,[3] M.S. Golden,[3] Yu-Zhong Zhang,[4] H.O. Jeschke,[4] R. Valentí,[4] A. Erb,[5] A. Gloskovskii,[6] and J. Fink,[1,2]

[1] *Helmholtz-Zentrum Berlin, Albert-Einstein-Strasse 15, 12489 Berlin, Germany*

[2] *Leibniz-Institute for Solid State and Materials Research Dresden, P.O.Box 270116, D-01171 Dresden, Germany*

[3] *Van der Waals-Zeeman Institute, University of Amsterdam, NL-1018XE Amsterdam, The Netherlands*

[4] *Inst. für Theor. Physik, Goethe-Universität, Max-von-Laue-Straße 1, 60438 Frankfurt, Germany*

[5] *Walther-Meissner-Institut, Walther-Meißner Strasse 8, 85748 Garching, Germany*

[6] *Institut für Anorganische Chemie und Analytische Chemie, Johannes Gutenberg-Universität, 55099 Mainz, Germany*

(Dated: October 1, 2009)

From a combination of high resolution angle-resolved photoemission spectroscopy and density functional calculations, we show that $BaFe_2As_2$ possesses essentially two-dimensional electronic states, with a strong change of orbital character of two of the Γ-centered Fermi surfaces as a function of k_z. Upon Co doping, the electronic states in the vicinity of the Fermi level take on increasingly three-dimensional character. Both the orbital variation with k_z and the more three-dimensional nature of the doped compounds have important consequences for the nesting conditions and thus possibly also for the appearance of antiferromagnetic and superconducting phases.

PACS numbers: 74.70.-b, 74.25.Jb, 79.60.-i, 71.20.-b

arXiv:0910.0147v1 [cond-mat.supr-con] 1 Oct 2009

Since the discovery of high T_c superconductivity in Fe-pnictides [1], many experiments have been carried out to reveal the physical and electronic properties of these materials [2, 3, 4, 5]. The parent compounds of Fe-pnictide superconductors are antiferromagnetic (AFM) metals. Both electron and hole doping suppresses the AFM order and leads to a superconducting phase. The AFM ordering is supposed to occur by nesting of hole pockets at the center of the Brillouin zone (BZ) and electron pockets at the zone corner. Nesting may be also important for the pairing mechanism in these compounds [6] although there are alternative scenarios based on the high polarizability of the As ions [7]. The nesting scenario could explain why in the SmFeAsO-based superconductors [8], predicted to have an almost two-dimensional electronic structure [9, 10], higher superconducting transition temperatures T_c are observed than in $BaFe_2As_2$-based systems [2] which are predicted to have a more three-dimensional electronic structure [11]. In general, reduction of the dimensionality increases the number of states that could be considered to be well nested. Furthermore, we point out that the orbital character of the states at the Fermi level E_F is very important for the nesting conditions as the interband transitions which determine the electronic susceptibility, as calculated by the Lindhard function, are (in weak coupling scenarios) by far strongest when the two Fermi surfaces have the same orbital character [12]. The admixture of three-dimensionality, arising from interlayer coupling, makes the materials potentially more useful in devices and other applications. Thus the dimensionality of the electronic structure, i.e., the k_z dispersion of the electronic states is of great importance for the understanding and application of these new superconductors.

Although angle-resolved photoemission spectroscopy (ARPES) is an ideal tool to study the dispersion of bands parallel and perpendicular to the FeAs layers there exist only a few experimental studies of these issues[13, 14, 15]. In this letter, we report a systematic study of the dimensionality of the electronic structure of $BaFe_{2-x}Co_xAs_2$ (x= 0 to 0.4) using polarization dependent ARPES, uncovering two new factors which are of great significance for the nesting of the Fermi surfaces of these systems. Firstly we show that the Co doping of $BaFe_2As_2$ strongly increases the three-dimensionality of the electronic structure. Secondly, we also detect an important change of the orbital character of the electronic states at the Fermi level when changing the wave vector perpendicular to the layers. Our results are in qualitative agreement with density functional theory (DFT) calculations.

Single crystals of $BaFe_{2-x}Co_xAs_2$, were grown in Amsterdam using a self-flux method. Another set of single crystals of $BaFe_2As_2$ were grown in Garching using Sn-flux. Characterizing studies on Amsterdam samples have been reported elsewhere [16]. The ARPES measurements were carried out at the BESSY II synchrotron radiation facility using the UE112-PGM2a beam line, equipped with a SCIENTA SES 100 analyzer. The total energy resolution was 25 meV while the angular resolution was 0.2° along the slit of analyzer and 0.3° perpendicular to it. All the samples were cleaved *in situ* at a temperature of less than 50 K. Further experimental details have been published previously [17]. Due to matrix element effects, measurements performed with polarized photons can detect different Fe 3d states depending on the polarization and sample alignment (i.e, Γ-X or Γ-M) (see Table I). In the following we will not discuss the xy

Table I: Sample alignment and Fe $3d$ orbitals which can be detected with s and p-polarized photons.

Alignment	Fe $3d_{x^2-y^2}$	Fe $3d_{z^2}$	Fe $3d_{xz}$	Fe $3d_{yz}$	Fe $3d_{xy}$
Γ-M (p-pol)	yes	yes	yes	no	no
Γ-M (s-pol)	no	no	no	yes	yes
Γ-X (p-pol)	no	yes	yes	yes	yes
Γ-X (s-pol)	yes	no	yes	yes	no

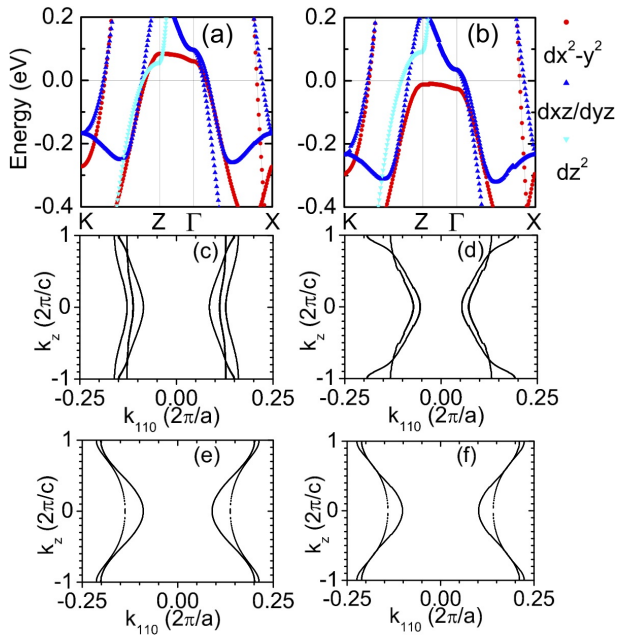

Fig. 1: (color online) Bands and their orbital character (a) for $BaFe_2As_2$ and (b) for $BaFe_{1.8}Co_{0.2}As_2$. (c) k_z dispersion around Γ for $BaFe_2As_2$ and (d) for $BaFe_{1.8}Co_{0.2}As_2$. (e) k_z dispersion around X for $BaFe_2As_2$ and (f) for $BaFe_{1.8}Co_{0.2}As_2$.

states as they are well below the Fermi energy E_F.

DFT calculations have been performed on $BaFe_2As_2$ and $BaFe_{1.8}Co_{0.2}As_2$, using the Perdew-Burke-Ernzerhof generalized gradient approximation (see Fig. 1). For $BaFe_2As_2$ experimental structural data were taken from [18]. For $BaFe_{2-x}Co_xAs_2$ we use Car-Parrinello molecular dynamics based on projector augmented wave basis to fully optimize the lattice structure within the virtual crystal approximation. High symmetry points of the BZ are denoted by Γ = (0, 0, 0), Z = (0, 0, 1), X = (1/2, 1/2, 0), and K = (1/2, 1/2, 1) in the units $(2\pi/a, 2\pi/a, 2\pi/c)$, where a and c are the tetragonal lattice constants of $BaFe_2As_2$ along the x and z axis, respectively. In Fig. 1(a) and (b), the orbital character of the bands is shown in color.

ARPES measurements on undoped $BaFe_2As_2$ are displayed in Fig. 2. The measurements were performed using the photon energies, hν=75 eV and hν=57 eV, corresponding to $k_z \approx 0$ (Γ point) and $k_z \approx 1$ (Z point), respectively. The k_z values are calculated using an inner potential of 15 eV [14]. s-polarized photons were used for recording the data along the Γ-X direction. Figure 2(b)-(e) depicts the hν=75 eV data. We observe a hole pocket at Γ and an electron pocket at X in the Fermi surface map. Figure 2(c) shows the energy distribution map taken along the k_{110} direction. We resolved two bands (α_1 and α_2) at Γ. Only α_1 crosses E_F while α_2 is not visible for binding energies less than 20 meV. A Fermi vector $k_F = 0.07 \pm 0.01$ Å^{-1} is calculated for α_1 by fitting the momentum distribution curve (MDC) taken over the integration range of a 20 meV window with respect to E_F. Using the polarization dependent selection rules (see Table I), with s-polarized photons along the Γ-X direction, the α_1 band can be attributed to $x^2 - y^2$ and the α_2 band is related to xz and yz states. Around Γ a weak spectral feature is observed near 100 meV below E_F. This feature is related to a back folding and hybridisation of bands near Γ and X, due to the AFM order in the As-Fe-As block. Around the zone corner X we observe two bands along k_{110} (α_2 and β_2) [Fig. 2(c)], and an additional hole pocket along k_{-110} (β_1) [Fig. 2(e)]. Maintaining the same geometry, but switching to hν=57 eV ($k_z \approx 1$) we can identify [Fig. 2(f)] two hole pockets around Γ and one electron pocket around X. The energy distribution map [Fig. 2(g)] shows two bands crossing E_F at the zone center (α_1 and α_2). Since there is no clear separation between these bands we give the average Fermi vector $k_F = 0.11 \pm 0.01$ Å^{-1}. The small difference in Fermi vectors between Γ and Z suggests a modest k_z dispersion in undoped $BaFe_2As_2$ a point which we will return to later.

Next we discuss our ARPES measurements on $BaFe_{1.6}Co_{0.4}As_2$. The data shown in Fig. 3 were recorded along Γ-X with hν=75 eV, corresponding to $k_z \approx 0$. Constant energy contours around Γ were taken with p-polarized photons [see Fig. 3(a)] and analogous contours around X were taken with s-polarized photons [Fig. 3(b)] because no spectral weight was observed at X with p-polarized photons. To resolve the band features we made different cuts along the k_{-110} direction at Γ and X. In Fig. 3(c) and (e) we can see that no bands cross E_F near Γ in these measurements performed with p-polarized photons. The final spectral weight observed in Fig. 3(a) at E_F is due to the tail of the top of the valence band. Using the polarization dependent selection rules of Table I, we can thus exclude hole pockets formed from states having z^2, xz, or yz character. The existence of hole pockets with $x^2 - y^2$ character, which according to the band structure calculations should be the first to sink below E_F upon electron doping, is excluded from measurements using s-polarized photons [Fig. 3(g)]. Therefore for high Co doping of $BaFe_2As_2$, the hole pockets for $k_z \approx 0$ are completely filled, i.e., there are no states at E_F near the Γ point. Similar conclusions were derived in a previous report [19] but without polarization analysis,

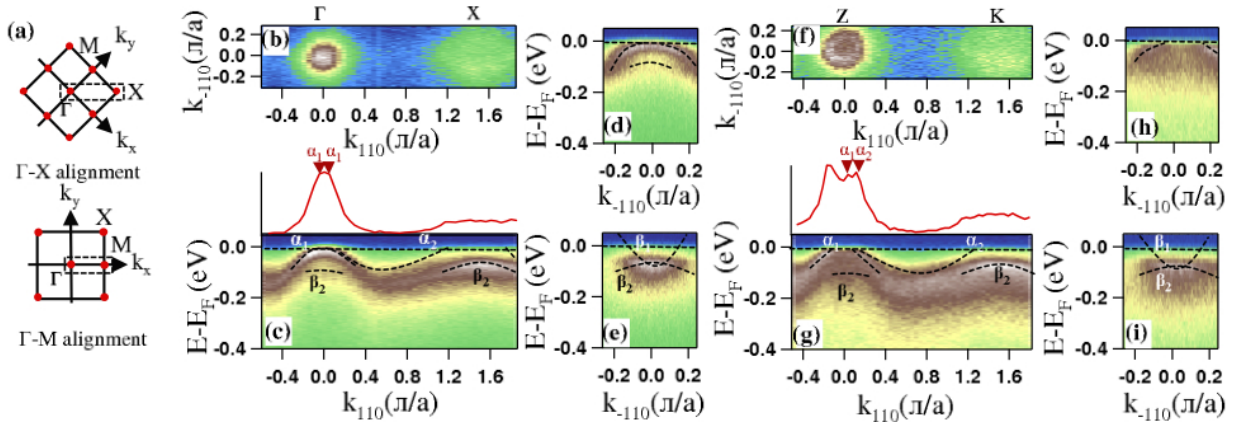

Fig. 2: (color online) ARPES data on undoped $BaFe_2As_2$ using s-polarized photons measured along Γ-X. (a) Cartoon of sample alignment and k space covered. (b)-(e) hν=75 eV, corresponding to $k_z \approx 0$ (Γ). (b) Fermi surface map, (c) energy distribution map (EDM) taken along the k_{110} direction, (d) EDM along k_{-110} around the Γ point and (e) around the X point. (f)-(i) Analogous data but taken with hν = 57 eV, corresponding to $k_z \approx 1$ (Z). The red curves in panel (c) and (g) represent momentum distribution curves at E_F.

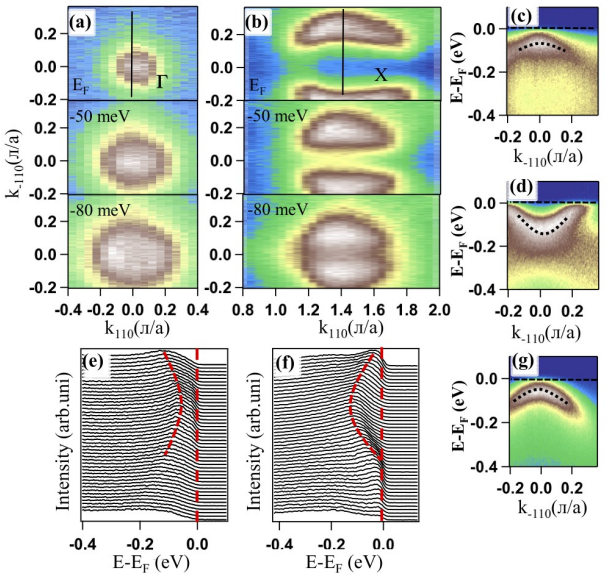

Fig. 3: (color online) $BaFe_{1.6}Co_{0.4}As_2$ARPES data along Γ-X. (a) and (b) constant energy maps near E_F, at E_F-50 meV, and E_F-80 meV around Γ and X, measured with p-polarized and s-polarized photons, respectively. (c) and (d) depict cuts taken along the k_{-110} direction from the center of Γ and X while (e) and (f) show the corresponding energy distribution curves. (g) as in panel (c) but measured with s-polarized photons.

the absence of a hole pocket at Γ cannot definitely be excluded. Furthermore, in $BaFe_{1.6}Co_{0.4}As_2$ the size of the electron pocket at X ($k_z \approx 0$) has become larger by a factor of two when compared to the undoped system. This indicates a shift of E_F to higher energies upon substituting Fe by Co. On the other hand, we point out that we were not able to perform a full integration of the volume of the Fermi cylinders to judge whether a Co atom really adds one full electron to the Fe 3d dominated low-energy band structure.

In order to reveal the k_z dispersion of the bands in $BaFe_2As_2$, we have performed photon energy dependent scans with excitation energies ranging from 75 eV to 150 eV in steps of 5 eV. Figure 4(a) depicts the Fermi surface map in the k_{100} vs. hν plane. The data were recorded along the Γ-M direction with p-polarized light. The strong and periodic intensity variation with k_z would at first sight seem to indicate a strong dispersion along this k direction. However, by fitting the MDCs we traced two bands across Γ and Z which are showing almost no or only minor k_z dispersion within our resolution limits. The clue to what is happening here comes from the DFT calculations. Inspection of Fig. 1(a) shows that near the Z point there is a z^2 related Fermi surface, while near Γ, only $x^2 - y^2$ and xz/yz states cross E_F. This radical k_z dependent change of the orbital character of the Fermi surface – which is naturally periodic in the c-axis reciprocal lattice vector – combined with the strong photon energy dependence of the matrix elements for emission from z^2 states [17] gives rise to the strong intensity variations shown here and reported in [13, 14, 15]. The true k_z dispersion for undoped $BaFe_2As_2$ between Γ and Z is small, as can also be seen from the DFT results of Fig. 1(c). Analogous ARPES data for $SrFe_2As_2$ and $EuFe_2As_2$ (not shown) confirm that the k_z dispersion derived from a careful MDC fit analysis for the $k_x = k_y = 0$ centered Fermi surfaces is small. Thus the picture for undoped $BaFe_2As_2$ is clear: there is little k_z dispersion of the states around $k_x = k_y = 0$, but there is an important k_z-dependent change in the orbital character of the Γ/Z-centerd Fermi surfaces.

Having dealt with the important question of the dimensionality and the orbital character of the central

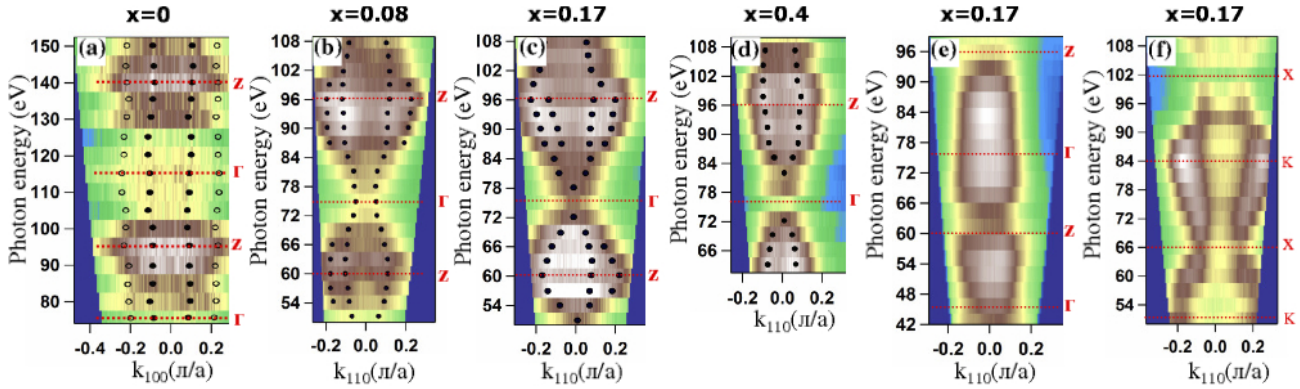

Fig. 4: (color online) Photon energy dependent ARPES measurements performed on $BaFe_{2-x}Co_xAs_2$ to reveal the k_z dispersion as a function of doping concentration. (a) Fermi surface for x=0, in the k_{100} vs. hν plane. (b), (c), and (d) Fermi surfaces in the k_{110} vs. hν plane, measured with p-polarized photons, for x=0.08, 0.17, and 0.4, respectively. (e) and (f) Fermi surface maps for x=0.17 measured with s-polarized photons around $k_x = k_y = 0$ and $k_x = k_y = 1$ respectively.

Fermi surface cylinders of the undoped parent compound $BaFe_2As_2$, we now address the issue of the evolution of the k_z dispersion in $BaFe_{2-x}Co_xAs_2$ as a function of Co doping concentration. Figures 4(b)-(d) show the Fermi surface maps in the k_{110} vs. hν plane, measured along Γ-X using p-polarized photons and photon energy steps of 3 eV. For lower Co concentrations, by fitting the MDCs, we could resolve two bands crossing E_F around Z while at x=0.4 only one band could be resolved. A remarkable observation is that with increasing Co concentration, the k_z dispersion increases and the spectral weight at Γ decreases. In the geometry used in Fig. 4(b)-(d), we probe xz, yz, and z^2 states. Thus we relate the outer bands to z^2 states while the inner ones to xz, yz states. In order to obtain more information on the orbital character of the bands, we contrast the x=0.17 data of Fig. 4(c), measured with p-polarization, with analogous data measured with s-polarization which are presented in Fig. 4(e). In the latter the spread of the spectral weight along the k_{110} direction is considerably reduced and the intensity is large at Γ and small at Z. Since in Γ-X (s-polarized) geometry, we do not detect z^2 states, and since at that doping level the $x^2 - y^2$ band is already completely filled [see also Fig. 1(b)], we observe here only the degenerate xz, yz bands. These states give rise to spectral weight at Γ but not at Z, as we have learned that these states transform at Z into z^2 states which cannot be detected in this geometry. Thus summarizing the situation for the states near the Γ point: with increasing doping concentration, first the $x^2 - y^2$ hole pocket will be filled at $x \approx$0.1 and later on the xz, yz hole pocket moves below E_F above $x \approx$0.2. At Z, the $x^2 - y^2$ pocket disappears near x=0.2 but there remains a hole pocket which has predominantly z^2 character. This means that with increasing doping concentration the system transforms from a more two dimensional system with strong nesting conditions to a more three-dimensional metal where nesting is in principle possible in the $k_z = \pm 1$ planes of the BZ, but there it is strongly reduced due to the different orbital character of the Fermi surfaces. In the k_z=0 plane nesting is no longer possible since there is no hole pocket. The observed doping dependence of the electronic structure is in remarkable agreement with the band structure calculations [Fig. 1 (c) and (d)]. Finally, we report for x=0.17 also a clear k_z dispersion along the X-K direction, derived from fits of MDCs of data shown in Fig. 4(f) where, due to this specific geometry, we probe all states (xz, yz, and $x^2 - y^2$) expected at E_F. The strength of the dispersion and the small difference in the dispersion for the three bands is in good qualitative agreement with the calculations presented in Fig. 1(f).

In conclusion, we have performed a systematic photon energy dependent high resolution ARPES study to reveal the intrinsic k_z dispersion in $BaFe_{2-x}Co_xAs_2$ compounds. In the undoped system we see a modest k_z dispersion near Γ indicating a more two-dimensional system. At higher Co doping the k_z dispersion increases and a gradual filling of all three hole pockets at Γ is detected. Thus in the region of the BZ near k_z=0 the nesting conditions are strongly reduced. In this context, our results on the orbital character indicate that nesting occurs predominantly in the k_z=0 plane since at the top and at the bottom of the BZ the orbital character of the Fermi cylinders in the center and in the corner is different ($x^2 - y^2$/ z^2 at Z and xz/ yz at K). Furthermore, the warped Fermi cylinders in optimally doped $BaFe_{2-x}Co_xAs_2$ could lead to nesting vectors which are pointing out of the Fe layers possibly leading to a more three-dimensional superconducting state. The present results could possibly lead to a microscopic understanding of the disappearance of AFM order upon doping for x=0.06 and the suppression of the superconducting phase in the overdoped phase near x=0.18 [20]. The results on the dimensionality have also implication for the potential application of these materi-

als.

[1] Y. Kamihara *et al.*, J. Am. Chem. Soc.**130**, 3296 (2008).
[2] M. Rotter *et al.*, Phys. Rev. Lett. **101**, 107006 (2008).
[3] X. F. Wang *et al.*, Phys. Rev. Lett. **102**, 117005 (2009).
[4] H. Q. Yuan *et al.*, Nature (London) **457**,565 (2009).
[5] M. A. Tanatar *et al.*, Phys. Rev. B **79**, 094507 (2009).
[6] I. I. Mazin *et al.*, Phys. Rev. Lett. **101**, 057003 (2008).
[7] G. A. Sawatzky *et al.*, Europhys. Lett. **86**, 17006 (2009).
[8] R. H. Liu *et al.*, Phys. Rev. Lett. **101**, 087001 (2008).
[9] D.J. Singh and M.-A. Du, Phys. Rev. Lett. **100**, 23700 (2008).
[10] F. Ma and Z.-Y. Lu, Phys. Rev. B **78**, 033111 (2008).
[11] D. J. Singh, Phys. Rev. B **78**, 094511 (2008).
[12] S. Graser *et al.*, New J. Phys. **11**, 025016 (2009).
[13] C. Liu *et al.*, Phys. Rev. Lett. **102**, 167004 (2009).
[14] P. Vilmercati *et al.*, Phys. Rev. B **79**, 220503 (R) (2009).
[15] T. Kondo *et al.*, arXiv:090502 (2009).
[16] F. Massee *et al.*, arXiv:0907.5544v1.
[17] J. Fink *et al.*, Phys. Rev. B **79**, 155118 (2009).
[18] Q. Huang *et al.*, Phys. Rev. Lett. **101**, 257003 (2008).
[19] Y. Sekiba *et al.*, New J. Phys. **11**, 025020 (2009).
[20] J.-H. Chu *et al.*, Phys. Rev. B **79**, 014506 (2009).